Supplementary Material (ESI) for Chemical Communications


# Supplementary Information: Energetics of Conformational Conversion between 1,1,2-Trichloroethane Polymorphs

*Maciej Bujak*[a], *Marcin Podsiadło*[b] *and Andrzej Katrusiak*[b]*

[a]Institute of Chemistry, University of Opole, Oleska 48, 45-052 Opole, Poland; [b]Faculty of Chemistry, Adam Mickiewicz University, Grunwaldzka 6, 60-780 Poznań, Poland

*E-mail: katran@amu.edu.pl

## 1. Experimental Methods

### 1.1 *In-situ* Low-Temperature and High-Pressure Crystal Growth

1,1,2-Trichloroethane was purchased (purrum, Fluka AG) and used without further purification. It was isobarically frozen in a glass capillary (internal diameter of 0.3 mm and 0.01 mm of wall thickness). The liquid sample filling 2 - 3 mm of the sealed capillary was cooled in a nitrogen gas stream from an Oxford Cryosystems attachment of a diffractometer. Setting the temperature of the gas stream of 170 K yielded a polycrystalline material, which was warmed up to the temperature of *ca.* 230 K. Growth of the single crystal was achieved by the cycling, at a rate of 1 $K \cdot min^{-1}$, within the range of 234 - 236 K reducing the number of crystal seeds left in each cycle. Eventually one seed grew in all the sample volume (M. Podsiadło, K. Dziubek, M. Szafrański and A. Katrusiak, *Acta Crystallogr*., Sect. B, 2006, **62**, 1090). The single-crystal X-ray intensity data were collected at 220 K, and then at 100 K.

The high-pressure freezing of single crystal of 112TCE was carried out in a modified Merrill-Bassett diamond-anvil cell, DAC (L. Merrill and W. A. Bassett, *Rev. Sci. Instrum.*, 1974, **45**, 290), with diamond anvils (culet diameter 0.8 mm) mounted on the hardened-steel seats (the opening angle *ca.* 60º). A general description of this high-pressure crystallization method was analogous to those

previously reported (R. J. Fourme, *Appl. Cryst.*, 1968, **1**, 23; W. L. Vos, L. W. Finger, R. J. Hemley and H. Mao, *Phys. Rev. Lett.*, 1993, **71**, 3150; D. R. Allan, S. J. Clark, M. J. P. Brugmans, G. J. Ackland and W. L. Vos, *Phys. Rev. B, Condens. Mat.*, 1998, **58**, R11809; M. Bujak, A. Budzianowski and A. Katrusiak, *Z. Kristallogr.*, 2004, **219**, 573) and is illustrated in Figure 1. The gasket was made of 0.3 mm thick steel foil with a 0.45 mm in diameter hole spark-eroded, and pre-indented to ca. 0.28 mm (A. Katrusiak, *J. Appl. Cryst.*, 1999, **32**, 1021). After nucleation the polycrystalline sample was heated with a hot-air gun until all but one crystallites melted. This seed was allowed to grow filling the disc-shaped chamber. The first data set was collected at 0.47(5) GPa. The conformational phase transition, between 0.47(5) and 1.20(5) GPa, was reflected in the changes in 112TCE crystals habit. The pressure in a DAC was determined from the ruby-fluorescence line shift using a BETSA PRL spectrometer, (J. D. Barnett, S. Block and G. J. Piermarini, *Rev. Sci. Instrum.*, 1973, **44**, 1; G. J. Piermarini, S. Block, J. D. Barnett and R. A. Forman, *J. Appl. Phys.*, 1975, **46**, 2774) with the accuracy of *ca.* 0.05 GPa.

### 1.2. Data Collection, Data Reduction and Refinement

The low-temperature/ambient (0.1 MPa)-pressure and room-temperature (295 K)/high-pressure diffraction data were collected on a KM-4 CCD diffractometer with the graphite-monochromated MoK$\alpha$ radiation. At 220 and 100 K the reflections were measured using the $\omega$-scan techniques with $\Delta\omega$ = 0.80 and 1.0º, and 20 and 15 s exposure times, respectively. The pressure-frozen single crystals of 112TCE were centred on the diffractometer by the shadow method (A. Budzianowski and A. Katrusiak, In *High-Pressure Crystallography*, A. Katrusiak and P. F. McMillan, Eds.; Kluwer Academic Publishers: Dordrecht, The Netherlands, 2004; pp. 101-112). The room temperature/high pressure intensity data, at 0.47(5), 1.20(5) and 1.91(5) GPa, were collected using the $\varphi$- and $\omega$-scan techniques with $\Delta\omega/\Delta\varphi$ = 0.7º and 25 s exposures.

All data were accounted for the Lorentz, polarization and sample absorption effects (Oxford Diffraction. *CrysAlis CCD, Data collection GUI for CCD and CrysAlis RED CCD data reduction GUI, versions 1.171.24 beta*, Wrocław, Poland, 2004; G. M. Sheldrick, *SHELXTL*. Siemens Analytical X-ray Instrument Inc.: Madison, WI, USA, 1990; A. Katrusiak, *REDSHABS*. Adam Mickiewicz University,

Poznań, Poland, 2003; A. Katrusiak, *Z. Kristallogr.*, 2004, **219**, 461) and the high-pressure data additionally for the absorption of the X-rays by DAC and shadowing of the single crystal by the gasket edges (A. Katrusiak, *REDSHABS*. Adam Mickiewicz University, Poznań, Poland, 2003; A. Katrusiak, *Z. Kristallogr.*, 2004, **219**, 461). All structures were solved by direct methods and refined with SHELX-97 (G. M. Sheldrick, *SHELX-97*. University of Göttingen, Göttingen, Germany, 1997). The Cl and C atoms were refined with anisotropic displacement parameters. The H-atoms were added using the standard geometric criteria, refined using the riding model with constrained C–H distances and $U_{eq}$*'s* equal for $CH_2$ and CH to 1.2 times $U_{eq}$*'s* of the corresponding C-atoms. The occupancy of the H-atoms was identical as those of their carriers. The *CrysAlis CCD* and *CrysAlis RED* programs (Oxford Diffraction. *CrysAlis CCD, Data collection GUI for CCD and CrysAlis RED CCD data reduction GUI, versions 1.171.24 beta*, Wrocław, Poland, 2004) were used for the data collection, unit-cell refinement and data reductions (initial reduction of the high-pressure intensity data). The 112TCE crystal data and structure determination summary are listed in Table S1. The bond lengths, angles and the shortest intermolecular distances are presented in Table S2.

**Table S1:** The 112TCE crystal data and structure determination summary.

| | | | | | |
|---|---|---|---|---|---|
| temperature, K | 220.0(1) | 100.0(1) | 295(2) | 295(2) | 295(2) |
| pressure | 0.1 MPa | 0.1 MPa | 0.47(5) GPa | 1.20(5) GPa | 1.91(5) GPa |
| formula | $C_2H_3Cl_3$ | $C_2H_3Cl_3$ | $C_2H_3Cl_3$ | $C_2H_3Cl_3$ | $C_2H_3Cl_3$ |
| fw, g/mol | 133.39 | 133.39 | 133.39 | 133.39 | 133.39 |
| crystal size, $mm^3$ | 0.30 x 0.20 x 0.20 | 0.30 x 0.20 x 0.20 | 0.44 x 0.44 x 0.25 | 0.44 x 0.44 x 0.24 | 0.44 x 0.44 x 0.23 |
| crystal system | monoclinic | monoclinic | monoclinic | monoclinic | monoclinic |
| space group[a], $Z$ | P 1 $2_1$/c 1, 4 | P 1 $2_1$/c 1, 4 | P 1 $2_1$/c 1, 4 | P 1 1 $2_1$/n, 4 | P 1 1 $2_1$/n, 4 |
| *a,* Å | 5.2875(7) | 5.1516(4) | 5.2539(19) | 5.0448(11) | 4.9978(15) |
| *b,* Å | 8.8172(11) | 8.5488(6) | 8.698(3) | 8.3551(18) | 8.208(3) |
| *c*, Å | 11.1861(12) | 11.3545(6) | 10.948(5) | 11.006(5) | 10.982(4) |
| $\beta$, º | 93.121(10) | 92.602(5) | 93.01(3) | | |
| $\gamma$, º | | | | 94.643(18) | 94.77(3) |
| $V$, $Å^3$ | 520.73(11) | 499.54(6) | 499.6(3) | 462.4(3) | 448.9(3) |
| $\rho$, $g/cm^3$ | 1.702 | 1.774 | 1.773 | 1.916 | 1.974 |
| $\mu$, $mm^{-1}$ | 1.582 | 1.649 | 1.648 | 1.781 | 1.835 |
| $\theta$ range, º | 2.94 – 25.22 | 2.98 – 25.24 | 2.99 – 25.23 | 4.46 – 25.24 | 3.11 – 25.20 |
| index ranges | $-5 \le h \le 6$ | $-4 \le h \le 6$ | $-6 \le h \le 6$ | $-6 \le h \le 6$ | $-5 \le h \le 5$ |
| | $-10 \le k \le 10$ | $-9 \le k \le 10$ | $-10 \le k \le 10$ | $-9 \le k \le 9$ | $-8 \le k \le 8$ |
| | $-13 \le l \le 13$ | $-13 \le l \le 13$ | $-6 \le l \le 6$ | $-3 \le l \le 3$ | $-9 \le l \le 9$ |
| reflns collected | 3086 | 3511 | 2798 | 2125 | 2469 |
| $R_{int}$ | 0.0426 | 0.0309 | 0.0941 | 0.1048 | 0.2060 |
| data [$I > 2\sigma(I)$] | 808 | 868 | 282 | 131 | 337 |
| data/parameters | 939/65 | 904/46 | 288/46 | 231/46 | 353/46 |
| GOF on $F^2$ | 1.085 | 1.252 | 1.179 | 0.988 | 1.182 |
| $R_1$ [$I > 2\sigma(I)$] | 0.0547 | 0.0287 | 0.0566 | 0.0488 | 0.0419 |
| $R_1$ (all data)[b] | 0.0659 | 0.0302 | 0.0572 | 0.0762 | 0.0594 |
| $wR_2$ (all data)[b] | 0.1386 | 0.0554 | 0.1463 | 0.1028 | 0.1151 |
| lrgst diff peak, $e/Å^3$ | 0.448 | 0.304 | 0.156 | 0.197 | 0.247 |
| lrgst diff hole, $e/Å^3$ | –0.344 | –0.250 | –0.131 | –0.204 | –0.246 |

[a]extended form of the space group symbols has been given to underline a non-conventional setting of space group $P2_1/n$ (see the text), [b]$R1 = \Sigma||F_o|-|F_c||/\Sigma|F_o|$; $wR_2 = \{\Sigma[w(F_o^2-F_c^2)^2]/\Sigma[w(F_o^2)^2]\}^{1/2}$; $w = 1/[\sigma^2(F_o^2)+(aP)^2 + bP]$, where $P = (F_o^2 + 2F_c^2)/3$

**Table S2:** Molecular dimensions (Å, º) and the shortest intermolecular distances (Å) for 112TCE.

| Atoms; Pressure/Temperature (K) | | 0.1 MPa/220.0(1) | 0.1 MPa/100.0(1) | 0.47(5) GPa/295(2) | 1.20(5) GPa/295(2) | 1.91(5) GPa/295(2) |
|---|---|---|---|---|---|---|
| C11–Cl1/C12–Cl3 | C1–Cl1 | 1.810(6)/1.78(3) | 1.791(2) | 1.757(10) | 1.81(3) | 1.782(5) |
| C11–Cl2/C12–Cl2 | C1–Cl2 | 1.788(6)/1.97(3) | 1.782(2) | 1.794(16) | 1.78(2) | 1.775(5) |
| C11–C21/C12–C22 | C1–C2 | 1.458(8)/1.49(4) | 1.505(3) | 1.49(5) | 1.29(8) | 1.489(9) |
| C21–Cl3/C22–Cl1 | C2–Cl3 | 1.785(5)/1.80(3) | 1.7902(19) | 1.735(9) | 1.86(3) | 1.782(5) |
| C11–C21–Cl3/C12–C22–Cl1 | C1–C2–Cl3 | 109.9(4)/110(2) | 110.12(14) | 113(2) | 116(2) | 113.3(3) |
| C21–C11–Cl1/C22–C12–Cl3 | C2–C1–Cl1 | 107.1(4)/107(2) | 107.38(14) | 110(2) | 114(2) | 112.1(3) |
| C21–C11–Cl2/C22–C12–Cl2 | C2–C1–Cl2 | 112.5(4)/93(2) | 112.26(14) | 110.8(10) | 116(3) | 112.6(3) |
| Cl1–C11–Cl2/Cl3–C12–Cl2 | Cl1–C1–Cl2 | 110.6(3)/118.0(16) | 109.31(11) | 113.1(9) | 109(2) | 109.5(3) |
| Cl1–C11–C21–Cl3/Cl3–C12–C22–Cl1 | Cl1–C1–C2–Cl3 | –177.8(3)/174.4(15) | –177.44(10) | –179.9(4) | 64(2) | 61.1(4) |
| Cl2–C11–C21–Cl3/Cl2–C12–C22–Cl1 | Cl2–C1–C2–Cl3 | 60.6(5)/–65(2) | 62.39(17) | 54.6(15) | –63(2) | –62.9(4) |
| | Cl1···Cl3$^{I/II}$ | – | – | 3.466(6) | 3.414(11) | 3.389(2) |
| | Cl1···Cl3$^{III}$ | – | – | – | – | 3.487(2) |
| | Cl2···Cl2$^{IV}$ | – | – | – | 3.478(12) | 3.459(2) |
| | Cl2···Cl3$^{V}$ | – | – | – | – | 3.483(2) |
| | Cl3···C1$^{VI}$ | – | – | – | – | 3.398(4) |
| | Cl1···H11$^{VII}$ | – | – | – | 2.86 | 2.79 |
| Cl1···H12$^{VII}$ | | 2.91 | – | – | – | – |
| | Cl2···H21$^{V}$ | – | – | – | – | 2.95 |
| | Cl2···H21$^{VI}$ | – | – | – | – | 2.93 |
| | Cl3···H11$^{VI}$ | – | – | – | 2.83 | 2.74 |
| | Cl3···H22$^{VII}$ | – | – | – | – | 2.91 |

Symmetry codes: (I) –1 + x, 1/2 – y, –1/2 + z; (II) 1/2 – x, 1/2 – y, –1/2 + z; (III) 1/2 + x, 1/2 + y, 1/2 – z; (IV) 2 – x, –y, –z; (V) 1/2 + x, –1/2 + y, 1/2 – z; (VI) –1/2 + x, –1/2 + y, 1/2 – z; (VII) –1 + x, y, z.

### 1.3. Compressibility Measurements

The compressibility measurement, between ambient pressure and ca. 1 GPa, was performed in the cylinder-and-piston apparatus (B. Baranowski and A. Moroz, *Polish J. Chem.*, 1982, **56**, 379). The pressure was changed at the rate of 0.02 GPa. The initial volume of the reaction chamber was 9.8 $cm^3$.

### 1.4. Quantum Mechanical Calculations

Geometry optimization (the torsion angles were kept as in crystal) and the subsequent volume calculations for both *gauche*$^-$ (at 295 K/0.47 GPa) and *transoid* (at 295 K/1.20 GPa) conformations of

112TCE were performed using the GAUSSIAN03 program package (M. J. Frisch, G. W. Trucks, H. B. Schlegel, G. E. Scuseria, M. A. Robb, J. R. Cheeseman, J. A. Montgomery, T. Vreven, K. N. Kudin, J. C. Burant, J. M. Millam, S. S. Iyengar, J. Tomasi, V. Barone, B. Mennucci, M. Cossi, G. Scalmani, N. Rega, G. A. Petersson, H. Nakatsuji, M. Hada, M. Ehara, K. Toyota, R. Fukuda, J. Hasegawa, M. Ishida, T. Nakajima, Y. Honda, O. Kitao, H. Nakai, M. Klene, X. Li, J. E. Knox, H. P. Hratchian, J. B. Cross, C. Adamo, J. Jaramillo, R. Gomperts, R. E. Stratmann, O. Yazyev, A. J. Austin, R. Cammi, C. Pomelli, J. W. Ochterski, P. Y. Ayala, K. Morokuma, G. A. Voth, P. Salvador, J. J. Dannenberg, V. G. Zakrzewski, S. Dapprich, A. D. Daniels, M. C. Strain, O. Farkas, D. K. Malick, A. D. Rabuck, K. Raghavachari, J. B. Foresman, J. V. Ortiz, Q. Cui, A. G. Baboul, S. Clifford, J. Cioslowski, B. B. Stefanov, G. Liu, A. Liashenko, P. Piskorz, I. Komaromi, R. L. Martin, D. J. Fox, T. Keith, M. A. Al-Laham, C. Y. Peng, A. Nanayakkara, M. Challacombe, P. M. W. Gill, B. Johnson, W. Chen, M. W. Wong, C. Gonzalez and J. A. Pople, *GAUSSIAN*03, Gaussian, Inc., Pittsburgh PA, 2003) at the HF/6–31+G* and HF/6–311++G** levels of theory.

## 2. Intermolecular Interactions in 1,1,2-Trichloroethane

The intramolecular distances at high pressures are comparable to those found in the phase $\alpha$ (Table S2). The intermolecular distances show some changes which, at the different temperature/pressure points, can be easily compared using the two-dimensional diagrams – the fingerprint plots (S. K. Wolff, D. J. Grimwood, J. J. McKinnon, D. Jayatilaka, N. A. Spackman, *CrystalExplorer* 2.0 (r 313). University of Western Australia, Perth, Australia, 2007; http://hirshfeldsurface.net/CrystalExplorer/; J. J. McKinnon, M. A. Spackman, A. S. Mitchell, *Acta Cryst*., Sect. B, 2004, **60**, 627; Figure S1). Lowering temperature and increasing pressure decreased Cl···Cl (the central red line) and Cl···H (the turquoise/blue 'wings') and increased density, which affect fingerprint plots of 112TCE (clear shifts of $d_e$ and $d_i$ to lower values). Surprisingly, there is no H···H interactions, shorter than the sum of two van der Waals radii, even at the highest pressure of 1.91 GPa which is a consequence of the molecular composition and the location of H-atoms in the 112TCE. The observation that more of the weak

intermolecular interactions are formed at high pressure is consistent with results observed in other high-pressure studies, for example on 1,1-dichloroethane (M. Bujak, M. Podsiadło and A. Katrusiak, *J. Phys. Chem.*, 2008, **B112**, 1184) where high pressure induces Cl···Cl interactions at *ca.* 1.5 GPa.

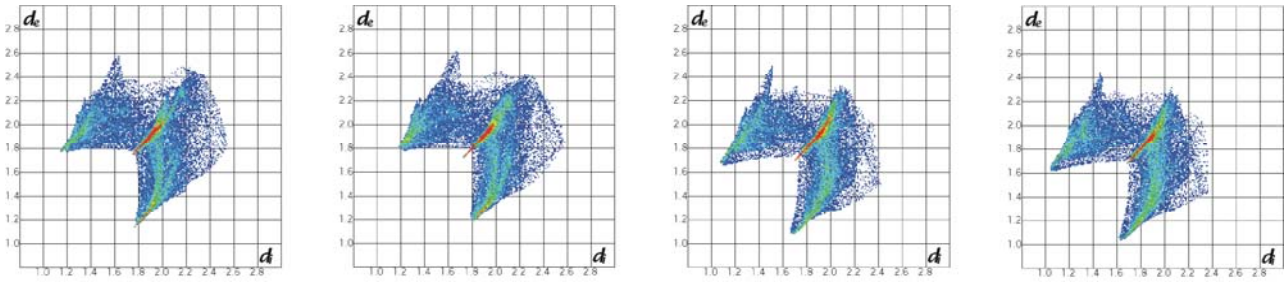

(a) (b) (c) (d)

**Figure S1.** Two-dimensional fingerprint plots for the structures of 112TCE at: (a) 100 K/0.1MPa; (b) 295 K/0.47 GPa; (c) 295 K/1.20 GPa; and (d) 295 K/1.91 GPa.

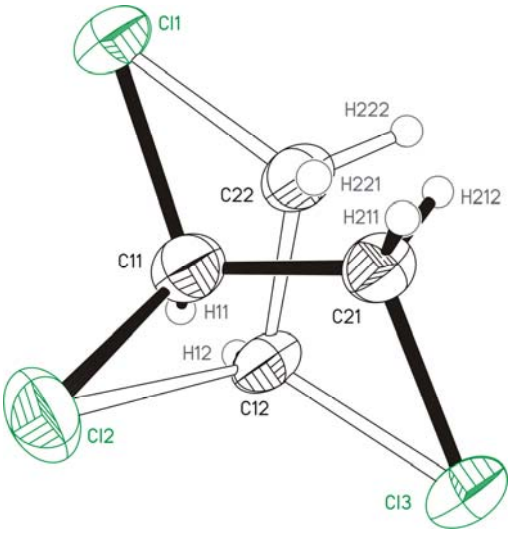


**Figure S2.** The disordered molecule of 112TCE at 220 K/0.1 MPa - phase *α*. Displacement ellipsoids are plotted at the 25% probability level.

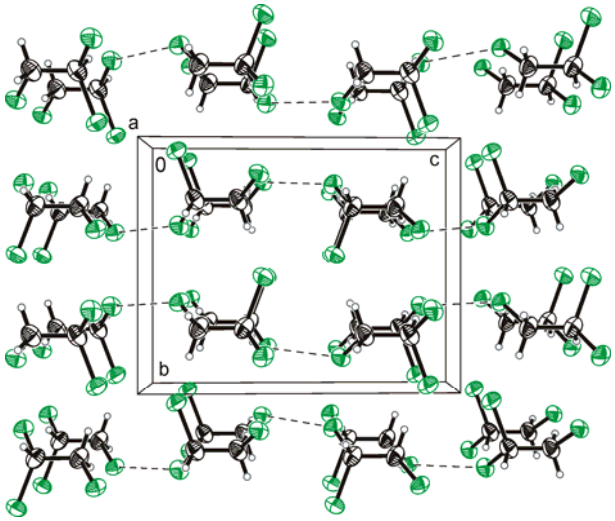


**Figure S3.** The crystal structure of 112TCE at 295 K/0.47 GPa along its *a*-axis. The dashed lines indicate the shortest Cl···Cl intermolecular contacts (Table S2). Displacement ellipsoids are plotted at the 25% probability level.

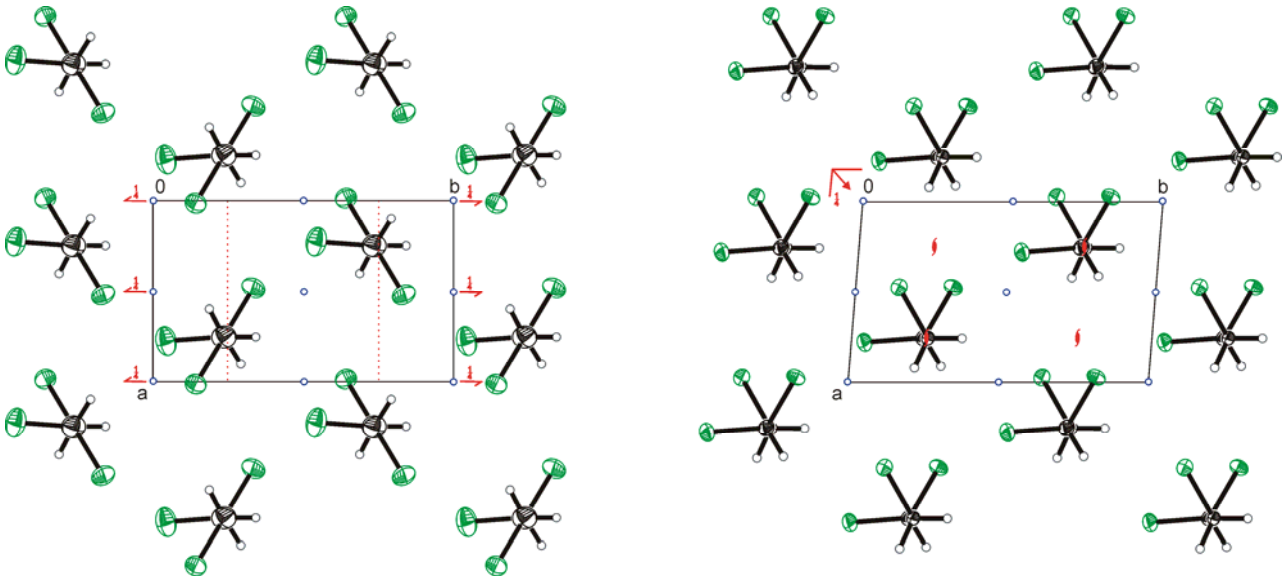


(a) (b)

**Figure S4**. The structure of 112TCE in the low-temperature/low pressure $P12_1/c1$ at 295 K/0.47 GPa phase $\alpha$ (a) and high-pressure $P112_1/n$ at 295 K/1.20 GPa phase $\beta$ (b), along their *c*-axes. Displacement ellipsoids are plotted at the 25% probability level. The positions of the glide planes, screw axes and the inversion centres are indicated.